# Optimum Filter Bandwidths for Optically Preamplified NRZ Receivers

Peter J. Winzer, *Associate Member, IEEE, Member, OSA*, Martin Pfennigbauer, *Student Member, IEEE*, Martin M. Strasser, *Student Member, IEEE*, and Walter R. Leeb, *Member, OSA*

***Abstract*—We present a comprehensive treatment of optically preamplified direct detection receivers for non-return-to-zero (NRZ) and return-to-zero (RZ) on/off keying modulation, taking into account the influence of different (N)RZ optical pulse shapes, specified at the receiver input, and filter transfer functions; optical Fabry–Pérot filters (FPFs) and Bragg gratings as well as electrical fifth-order Bessel and first-order $RC$ low-pass filters are considered. We determine optimum optical and electrical filter bandwidths and analyze the impact of bandwidth deviations on receiver sensitivity. Optimum receiver performance relies on a balance between noise and intersymbol interference (ISI) for NRZ transmission, while for RZ reception detection noise has to be traded against filter-induced signal energy rejection. Both for NRZ and 33% duty cycle RZ, optical filter bandwidths of around twice the data rate are found to be optimum. Receivers using RZ coding are shown to closely approach the quantum limit, and thus to outperform NRZ-based systems by several decibels. We further analyze the impact of important degrading effects on receiver sensitivity and optimum receiver bandwidths, including receiver noise, finite extinction ratio, chirp, and optical carrier frequency (or optical filter center frequency) fluctuations.**

***Index Terms*—Chirp, extinction ratio, frequency control, intersymbol interference (ISI), non-return-to-zero (NRZ), optical amplifiers, optical filters, return-to-zero (RZ), sensitivity.**

## I. Introduction

With the large-scale commercial deployment of erbium-doped fiber amplifiers (EDFAs), optically preamplified receivers have become the technically most practicable way of achieving (nearly) quantum-limited receiver performance in the 1.5-$\mu$m wavelength range [1]. By establishing the connection between optically preamplified receivers and classical square-law detectors, it was shown that the optimum optically preamplified receiver should employ a matched optical filter [2], [3]. Owing to technological constraints, however, the optical bandpass filter following the EDFA to reduce the amplified spontaneous emission (ASE) power at the detector always had to be taken much broader than the bandwidth of the data signal [3], [4]. In various analyses of optically preamplified receivers, the optical filter had therefore been assumed to let the data signal pass undistorted [5]–[10]. However, i) the increase of data rates into the 10–40-Gb/s range, ii) the growing availability of optical filters with bandwidths down to about 10 GHz, and iii) the employment of return-to-zero (RZ) coding have led to technically realizable situations in which narrow optical filter bandwidths start to deteriorate receiver performance by introducing optical-filter-induced signal distortions. Hence, a few analyses appeared that include, both on signal *and* noise,[1] the influence of Fabry–Pérot optical filters for non-return-to-zero (NRZ), ON–OFF keying (OOK) transmission [11]–[13]. Widely differing optimum optical filter bandwidths, ranging from 3.7 to 8 times the data rate, are given in these references for the simplifying case of rectangular data signals and integrate-and-dump electrical postdetection filters. Only reference [14] includes realistic (NRZ) optical pulse shapes and (third-order Butterworth) electrical filter characteristics, arriving at an optimum optical bandwidth of about 1.2 times the data rate. Reference [15], on the other hand, treats the filtering action of arrayed waveguide grating routers, both for NRZ and RZ rectangular optical pulse shapes and first-order $RC$ electrical low-pass filters, resulting in an optimum optical filter bandwidth of 0.9 times the data rate for the case of NRZ transmission.

The aim of this paper is threefold. First, we give optimum values for optical and electrical filter bandwidths for various typical optically preamplified receiver configurations, both for NRZ *and* RZ reception, using optical pulse shapes with $\cos^2$-shaped edges specified at the receiver input, as well as realistic filter characteristics; the optical filter is modeled either as a Fabry–Pérot filter (FPF) or as a fiber Bragg grating (FBG), and the electrical filter is assumed either a first-order $RC$ low-pass or a fifth-order Bessel filter. Second, we explain in depth the (different) degrading mechanisms that determine receiver performance for NRZ and RZ; we both qualitatively and quantitatively show that for NRZ systems, a tradeoff between receiver noise and intersymbol interference (ISI) has to be made, while RZ systems rely on a compromise between noise and filter-induced signal energy reduction. Third, we discuss and interpret the influence of some important imperfections (receiver noise, extinction ratio, chirp, frequency drift) on receiver performance as well as on the optimum receiver bandwidths. The analysis of optically preamplified receivers for RZ coding is particularly interesting, since recent experimental [16]–[18] and theoretical [16], [19], [20] work has shown that the sensitivity of direct detection optical receivers can be improved by several decibels in terms of average received power using RZ instead of NRZ, even if the (electrical) receiver bandwidth is only

Manuscript received October 20, 2000. This work was supported by the Austrian Science Fund (FWF) under Project P13998TEC and by the Austrian Academy of Sciences under Grant 754/99.

P. J. Winzer is with Bell Laboratories, Lucent Technologies, Holmdel, NJ 07733 USA (e-mail: pwinzer@ieee.org).

M. Pfennigbauer, M. M. Strasser, and W. R. Leeb are with the Institut für Nachrichtentechnik und Hochfrequenztechnik, Technische Universität Wien, Wien A-1050, Vienna, Austria.

Publisher Item Identifier S 0733-8724(01)07753-2.

[1]Note that—apart from the signal—the noise terms in an optically preamplified receiver are also influenced by the optical filter characteristics; for optical filters with bandwidths on the order of the signal spectral width, the frequently used noise approximations [5] become inaccurate.

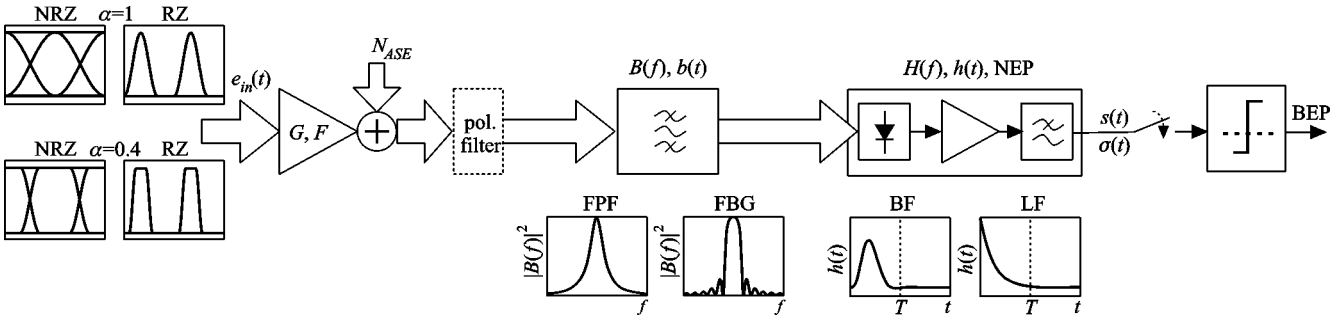


Fig. 1. Optically preamplified receiver structure. The optical (N)RZ input field $e_{\rm in}(t)$ (cf. optical power eye diagrams) is optically preamplified (gain $G$, noise figure $F$) and corrupted by amplified spontaneous emission (ASE). In addition to an optical bandpass filter [Fabry–Pérot filter (FPF), or fiber Bragg grating (FBG)] with power transmission $|B(f)|^2$, a polarization filter may be employed to reduce ASE. The impulse response of the detection chain is assumed to have fifth-order Bessel (BF) or first-order $RC$ low-pass (LF) characteristics [impulse response $h(t)$]. Electronic noise is accounted for by a noise equivalent power (NEP). Sampling and threshold decision of the electric signal with mean $s(t)$ and variance $\sigma^2(t)$ leads to a bit error probability (BEP).

on the order of 0.7 times the data rate. The use of optimized RZ receivers will lead to significant system improvements, especially for space-borne laser communication systems, where neither dispersion nor nonlinear effects set a lower limit on the RZ pulse duration, and where utmost receiver sensitivity in combination with a robust receiver setup is the prime goal [21]–[25].

The paper is organized as follows. Section II presents our model for the optically preamplified receiver, specifying optical pulse shapes and optical and electrical filter characteristics. Section III details the employed calculation method. Section IV gives a qualitative explanation of the different tradeoffs to be made when optimizing bandwidths in an RZ and an NRZ receiver, respectively. Section V then quantitatively treats an ideal optically preamplified receiver, i.e., a receiver with ideal optical and electronic components, discussing separately the influence of different receive electronics (Section V-A), different optical pulse shapes (Section V-B), and different optical filters (Section V-C). Section VI incorporates the influence of electronic noise and nonideal optical amplifier characteristics (Section VI-A), of finite extinction ratios (Section VI-B), of optical pulse chirp (Section VI-C), as well as of frequency drifts of the optical carrier with respect to the optical filter's center frequency (Section VI-D). Finally, Section VII states the most relevant conclusions of this work.

## II. System Model

The structure of the modeled optically preamplified receiver is shown in Fig. 1. The optical input field is given by its equivalent baseband representation $e_{\rm in}(t)$ at the *receiver input*, incorporating all propagation influences (e.g., dispersion) on the transmit signal. The input field is normalized to let its squared magnitude yield the optical input power ($p_{\rm in}(t) = |e_{\rm in}(t)|^2$). The optical power waveform representing a single "1"-bit, $p_1(t)$ is specified within the time interval $[0,\ (1+\alpha)T_p]$ as

$$p_1(t) = \begin{cases} \frac{E_1}{2T_p}\left[1-\sin\left(\frac{\pi}{\alpha T_p}\left(\left|t-(1+\alpha)\frac{T_p}{2}\right|-\frac{T_p}{2}\right)\right)\right], \\ \qquad t\epsilon\{[0,\ \alpha T_p] \vee [T_p,\ (1+\alpha)T_p)]\} \\ \frac{E_1}{T_p}, \qquad t\epsilon[\alpha T_p,\ T_p] \end{cases} \tag{1}$$

where $E_1$ denotes the optical energy for a "1"-bit, $T_p$ is the effective pulse duration

$$T_p = \frac{\int_{-\infty}^{\infty} p_1(t)\,dt}{\max_t\{p_1(t)\}} = \frac{E_1}{\max_t\{p_1(t)\}} \tag{2}$$

and the parameter $\alpha$ specifies the pulse shape. Varying $\alpha$ from 1 to 0, the pulse changes from $\cos^2(t)$-like to rectangular. Logical "0"-bits are ideally represented by the absence of an optical signal; the employed model for finite extinction ratios will be explained in Section VI-B. Setting $T_p = T$ ($T$ being the bit duration) yields an isolated NRZ "1"-bit, while $T_p = d \cdot T$ produces RZ with duty cycle $d$. The results presented in this work are all based on pulses with $\alpha = 1$ and $\alpha = 0.4$ as well as on an RZ duty cycle of $d = 33\%$; the respective input signal eye diagrams for NRZ and RZ are given in Fig. 1.

The optical amplifier both amplifies the input field by $\sqrt{G}$ and adds a circularly symmetric complex Gaussian noise process, the ASE, with power spectral density [26]

$$N_{\rm ASE} = hcGF_{\rm equiv}/(2\lambda) \tag{3}$$

per spatial (and polarization) mode, where $hc/\lambda$ denotes the photon energy at wavelength $\lambda$, and $F \geq 2$ is the amplifier's noise figure. Note that $F$ may also include the influence of incoherent background light with power spectral density $N_b$ at the receiver input, which in fiber-based systems can be caused by the accumulated ASE of in-line optical amplifiers, and in free-space systems can be generated by an optical booster amplifier at the transmitter [37]. In this case, the additive noise process at the amplifier output can be specified by an equivalent noise figure $F_{\rm equiv}$ as

$$N_{\rm ASE} + GN_b = hcGF_{\rm equiv}/(2\lambda) \tag{4}$$

with

$$F_{\rm equiv} = F + 2N_b\lambda/(hc). \tag{5}$$

If the input signal's state of polarization is known (which is the case in, e.g., space-borne communications links), a polarization filter may optionally be employed, as indicated in Fig. 1, to reduce the number of ASE modes to a single one in a (usually spatially single-mode) system. The subsequent optical bandpass

filter with dimensionless, complex baseband field transfer function $B(f)$ and complex baseband impulse response $b(t)$ is assumed to be either a Fabry–Pérot filter (FPF) or a fiber Bragg grating (FBG), the latter in combination with a circulator to convert the FBG's bandstop characteristics into bandpass characteristics [30]. For an FPF, $B(f)$ is given in its Lorentzian approximation (which is valid for the practically relevant case of high etalon finesse) as [14], [29]

$$B_{\mathrm{FPF}}(f) = 1/(1 + j2f/\mathrm{FWHH}) \tag{6}$$

where FWHH denotes the filter's full width at half height or 3-dB bandwidth. For an FBG, we have [30]–[33]

$$B_{\mathrm{FBG}}(f) = \frac{1}{\tan[\kappa l]} \frac{-j\kappa \sin[\beta(f) l]}{j\beta(f)\cos[\beta(f) l] - (2\pi f/v_g)\sin[\beta(f) l]} \tag{7}$$

where $\beta(f)$ stands for

$$\beta(f) = \sqrt{(2\pi f/v_g)^2 - \kappa^2} \tag{8}$$

and $\kappa$ is the grating's coupling coefficient. In our simulations, $\kappa$ was kept constant at a typical value of 6 cm$^{-1}$ [30], while the length of the grating $l$ and the group velocity $v_g$ were appropriately set to achieve the desired FWHH at a constant sidelobe suppression ratio of 7 dB. The power transmission $|B(f)|^2$ of the two filters is shown in Fig. 1. Note that both the FPF and the FBG are normalized to unit peak transmission; any insertion loss $L$ of the optical filter can readily be accounted for, both for signal and noise, by using an effective optical amplifier gain of $GL$.

After optical filtering, the signal field is detected by means of a pin photodiode, mathematically described as a square-law device, followed by electrical preamplification and lowpass filtering. The impulse response of the entire electronics [transfer characteristics $H(f)$] is denoted $h(t)$ and is normalized to unit area,[2] $\int_{-\infty}^{\infty} h(t)\,dt = H(0) = 1$. In the frame of this work, the electronic circuitry is either assumed to have a first-order $RC$ low-pass characteristic or a fifth-order Bessel characteristic. The latter type of receive filter is widely used in optical receivers, even at data rates in the multigigabit-per-second regime, since it produces only little overshoot. The transfer function of the $RC$ low-pass filter (LF) is given by

$$H_{\mathrm{LF}}(f) = 1/\left(1 + j\pi f/(2B_h)\right) \tag{9}$$

where $B_h$ denotes the filter's power equivalent width [29]

$$B_h = \int_0^{\infty} |H(f)|^2\, df. \tag{10}$$

For the LF, the 3-dB bandwidth $B_{3\,\mathrm{dB}}$ is related to $B_h$ by $B_{3\,\mathrm{dB}} = 2B_h/\pi$. The transfer function of the Bessel filter (BF) is given by [19], [27]

$$H_{\mathrm{BF}}(f) = 945/(jf^5 + 15f^4 - 105jf^3 - 420f^2 + 945jf + 945). \tag{11}$$

[2]In the (in practice most likely) case of ac-coupled detection, this normalization reads $H(f_l) = 1$, where $f_l$ is the lower cutoff frequency of the receive electronics.

This filter's 3-dB bandwidth evaluates to $0.96B_h$. Electronic noise is specified by the detection chain's noise equivalent power (NEP); this quantity, usually given in $[\mathrm{W}/\sqrt{\mathrm{Hz}}]$, will be defined in (17) below [28]. Sampling and threshold decision of the electrical (analog) output signal with mean $s(t)$ and variance $\sigma^2(t)$ finally leads to a bit error probability (BEP).

## III. Calculation Method

To arrive at BEP results, we chose a quasi-analytical method. Given a pseudo-noise (PN) bit sequence of length $2^m - 1$, we generated the input optical field $e_{\mathrm{in}}(t)$ and calculated the signal's mean $s(t)$ at the decision gate according to [29]

$$s(t) = C\,|(e_{\mathrm{in}} * b)(t)|^2 * h(t) \tag{12}$$

where $C$ stands for the overall optoelectronic conversion factor ($[A/W]$ or $[V/W]$), and the symbol $*$ denotes a convolution

$$(x * y)(t) = x(t) * y(t) = \int_{-\infty}^{\infty} x(\tau) y(t-\tau)\, d\tau. \tag{13}$$

Neglecting both signal shot noise and ASE shot noise, whose variances are typically several orders of magnitude smaller than those of the beat noise terms between signal and ASE and between ASE with itself, the signal's variance $\sigma^2(t)$ reads [15], [19]

$$\sigma^2(t) = \sigma^2_{\text{s-ASE}}(t) + \sigma^2_{\text{ASE-ASE}} + \sigma^2_{\mathrm{elec}} \tag{14}$$

with the signal-ASE beat noise

$$\sigma^2_{\text{s-ASE}}(t) = 2C^2 N_{\mathrm{ASE}} \mathrm{Re}\left\{ \iint_{-\infty}^{\infty} e_{\mathrm{in}}(\tau) e^{\star}_{\mathrm{in}}(\tilde{\tau}) r_b(\tau - \tilde{\tau}) h(t-\tau) \cdot h(t-\tilde{\tau})\, d\tau\, d\tilde{\tau} \right\} \tag{15}$$

the ASE–ASE beat noise

$$\sigma^2_{\text{ASE-ASE}} = MC^2 N^2_{\mathrm{ASE}} \int_{-\infty}^{\infty} |r_b(\tau)|^2\, r_h(\tau)\, d\tau \tag{16}$$

and the noise of the electronic circuitry

$$\sigma^2_{\mathrm{elec}} = \mathrm{NEP}^2 C^2 B_h. \tag{17}$$

In these equations

$$r_b(t) = \int_{-\infty}^{\infty} b(\tau) b^{\star}(\tau - t)\, d\tau \tag{18}$$

denotes the optical filter's autocorrelation function [with the same notation for the electrical filter's autocorrelation $r_h(t)$], and $M$ specifies the number of (spatial and polarization) ASE modes.

With the expressions for signal and noise at hand, the BEP at a sampling time offset $t_s$ and for a decision threshold $s_{\mathrm{th}}$ reads

$$\mathrm{BEP}\,(t_s,\, s_{\mathrm{th}}) = \frac{1}{2^m - 1} \cdot \left\{ \sum_{k_0} \frac{1}{2} \mathrm{erfc}\left[ \frac{s_{\mathrm{th}} - s(t_s + k_0 T)}{\sqrt{2}\,\sigma(t_s + k_0 T)} \right] + \sum_{k_1} \frac{1}{2} \mathrm{erfc}\left[ \frac{s_1(t_s + k_1 T) - s_{\mathrm{th}}}{\sqrt{2}\,\sigma(t_s + k_1 T)} \right] \right\} \tag{19}$$

where the indexes $k_0$ and $k_1$ are used to distinguish between the $2^{m-1}-1$ transmitted "0"-bits and the $2^{m-1}$ "1"-bits of the PN sequence.[3] In the frame of this work, we will be interested in the optimum BEP values only, obtained by minimizing (19) with respect to $t_s$ and $s_{\rm th}$.

In (19), Gaussian signal statistics are assumed. This frequently employed assumption significantly simplifies numerical calculations by allowing the use of the complementary error function

$$\operatorname{erfc}(x) = \frac{2}{\sqrt{\pi}} \int_x^\infty \exp(-t^2)\, dt. \tag{20}$$

It has been shown [9], [34], [35] that the Gaussian approximation yields very accurate results in the case of OOK modulation, with predicted receiver sensitivities typically 0.2 to 0.5 dB worse than the exactly calculated ones. That this statement will hold over a wide range of receiver bandwidths can be expected from the results of [13], [36][44].

Finally, the receiver sensitivity $n_s$ is calculated, defined as the required average number of photons per bit at the optical amplifier input to achieve BEP $= 10^{-9}$; unless stated otherwise, the results presented in this work are given in terms of a sensitivity penalty $\gamma_q$ relative to the quantum limit $n_q$

$$\gamma_q = 10 \log(n_s/n_q) \quad [\text{dB}] \tag{21}$$

where $n_q$ evaluates to 41.0 photons/bit using the Gaussian approximation with optimized decision threshold.[4]

## IV. Tradeoffs for Optimum Receiver Bandwidths

Optimizing optical and electrical filter bandwidths in an optically preamplified receiver is a process of trading several degrading effects with different significance for NRZ and RZ signaling. The *optical filter* primarily serves to reject ASE, thus reducing the signal-independent ASE-ASE beat noise component $\sigma^2_{\text{ASE-ASE}}$, which is normally important for the detection of "0"-bits only. If chosen too narrow, however, the optical filter can introduce severe ISI to NRZ signals, with the adverse effects of closing the eye and—even more important—of raising the "0"-bit noise level due to "0"-bit signal-ASE beat noise. For RZ signals, on the other hand, optically induced ISI is typically no issue; too narrow-band optical filtering rather causes significant portions of the input pulse energy to be rejected, leading to lower electrical signal amplitudes and thus to worse receiver performance. A similar situation is found for the *electrical filter*, used to reduce all detection noise terms of (14). For NRZ, a balance between noise and ISI has to be sought, while for RZ, again, a compromise between noise and signal amplitude reduction due to too narrow-band filtering is aimed at; a degrading effect of ISI is usually *not* encountered at optimized receiver bandwidths for RZ with sufficiently small duty cycle, since at low bandwidths the signal power decreases more rapidly than the signal-independent noise $\sigma^2_{\text{ASE-ASE}} + \sigma^2_{\text{elec}}$ [20], so that the influence of signal-independent noise limits receiver performance well before ISI sets in.[5]

Generally, we anticipate at this point that broader than optimum filtering is to be preferred to too narrow filtering, since the degrading effect of increasing noise power is less severe than either introducing ISI or spectrally truncating the signal.

The qualitative description given here for the effects determining the optimum receiver bandwidths will be demonstrated and underlined by the following quantitative analyses.

## V. Ideal Receiver

In this section, we discuss the dependence of the receiver sensitivity as a function of both optical and electrical filter bandwidths for various *ideal* optically preamplified receiver setups; for given optical and electrical filter characteristics, the ideal receiver is specified by $M = 1$ (i.e., a single-mode system including polarization filtering), $F = 3$ dB, and $G$ sufficiently large to let $\sigma^2_{\text{s-ASE}}(t) + \sigma^2_{\text{ASE-ASE}}$ always dominate $\sigma^2_{\text{elec}}$.

### A. Different Receive Electronics' Transfer Functions

Fig. 2 shows, as a first example, the sensitivity penalty $\gamma_q$ [cf. (21)] relative to the quantum limit as a function of both the optical and the electrical bandwidth. The optical bandwidth is given as an FWHH normalized to the data rate $R$, and the axes representing the electrical bandwidth are scaled both in terms of a normalized power equivalent width ($B_h/R$, upper axes) and in terms of a 3-dB bandwidth ($B_{3\text{ dB}}/R$, lower axes). The underlying scenario comprises NRZ transmission with $\alpha = 1$ and an FPF for optical filtering. While Fig. 2 (a) is obtained using a BF in the electrical domain, Fig. 2(b) applies to an LF. The contour lines are separated by 0.25 dB. The two pairs of thick lines represent the optimum optical bandwidths for fixed electrical bandwidths (left to right), and the optimum electrical bandwidths for fixed optical bandwidths (top to bottom). Their intersection gives the globally optimum optical/electrical bandwidth constellation, which is quite different for the two receiver electronics. For identical bandwidths, the BF impulse response is temporally more confined and thus produces significantly less ISI. The BF power equivalent width can therefore be chosen as narrow as $0.8R$, while the optimum LF bandwidth amounts to $1.6R$ ($1 \cdot R$ in terms of $B_{3\text{ dB}}$). For RZ, on the other hand, the difference between BF and LF is not as pronounced, since it is not ISI but signal energy rejection that determines the optimum receiver setup in this case. To quantitatively express the influence of ISI on the optimum electrical bandwidth, we compared the results for a PN sequence with the sensitivity values found for a single "1"-bit (i.e., without allowing ISI effects) using NRZ with $\alpha = 1$ and optical FPF filtering. At $B_h = 0.8R$, an electrical-filter-induced ISI penalty of 0.9 dB was found for the BF, and as much as 1.9 dB for the LF.

Reducing ISI by broadening the LF must, on the other hand, be accompanied by narrowing the optical filter to compensate

[3]For the results presented here, a PN sequence with $m = 7$ proved sufficiently long to incorporate all relevant bit combinations producing ISI [20].

[4]The frequently cited value of 42.0 photons/bit is obtained if a computationally much simpler, but slightly suboptimum threshold is employed [34]. Note that somewhat different results for $\gamma_q$ as a function of the receiver bandwidths may be obtained if the receiver sensitivity is defined by other BEP values, since these require other input power levels, which, in turn, can give rise to different ratios of signal-dependent to signal-independent noise.

[5]If the signal-dependent noise term $\sigma^2_{\text{s-ASE}}(t)$ were the only one present, the electrical filter could be chosen still narrower; the optimum electrical bandwidth would then be solely determined by ISI, as explained in [20].

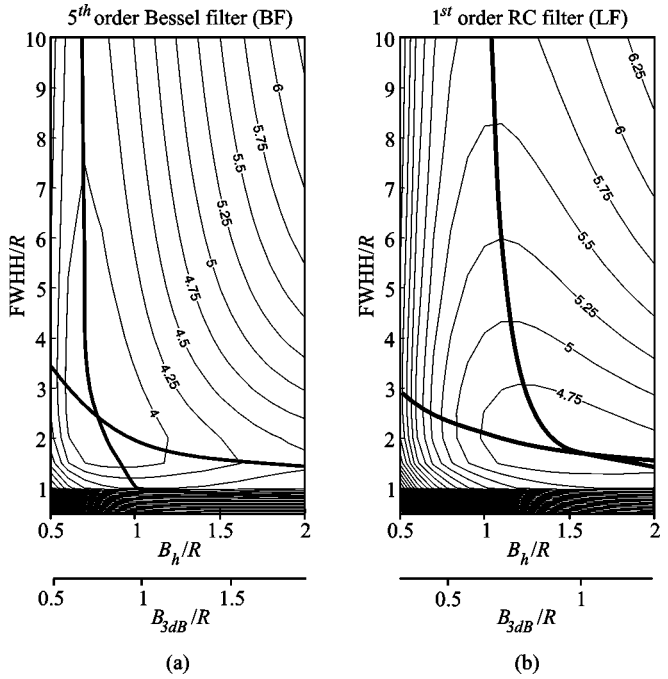


Fig. 2. Sensitivity penalty $\gamma_q$ relative to the quantum limit as a function of the optical filter 3-dB bandwidth (FWHH) and the electrical filter power equivalent bandwidth ($B_h$) and 3-dB bandwidth ($B_{3\,\mathrm{dB}}$), all normalized to the data rate $R$. NRZ transmission with $\alpha = 1$ and FPF optical filtering is considered. (a) and (b) apply to BF and LF electrical filtering, respectively. The contour lines are separated by 0.25 dB. The two pairs of thick lines represent the optimum optical bandwidths for fixed electrical bandwidths (left to right), and the optimum electrical bandwidths for fixed optical bandwidths (top to bottom).

for the increased detection noise until a new balance between noise and (both optical and electrical-filter-induced) ISI is established; the optimum FWHH in Fig. 2(b) is thus $1.7R$, while it is $2.4R$ in Fig. 2(a). However, even for optimized bandwidths, the LF option performs 0.8 dB worse than the BF realization. The advantage of using more sophisticated Bessel electrical filtering is less for RZ signaling, where it typically amounts to 0.2 dB.

### *B. Different Input Pulse Shapes*

Fig. 3 visualizes the influence of different input pulse shapes on ideal receivers with FPF optical filtering and BF electrical filtering. Fig. 3(a) and (c) give the sensitivity penalties relative to the quantum limit for NRZ with $\alpha = 1$ and $\alpha = 0.4$, respectively, while Fig. 3(b) and (d) apply to RZ with $\alpha = 1$ and $\alpha = 0.4$. The optimum bandwidth constellations are indicated by crosses. The most striking difference between the four plots is the RZ sensitivity gain [15], [16], [19], [20]. Using RZ coding instead of NRZ, one arrives at a sensitivity enhancement of 3.6 dB for $\alpha = 1$ and of 1.0 dB for $\alpha = 0.4$ at optimized bandwidths. Comparing NRZ with $\alpha = 0.4$ and RZ with $\alpha = 1$ and $d = 33\%$, two signaling formats with approximately the same rise and fall times, we find an RZ sensitivity gain of 1.2 dB. Further, it is evident from the figure that RZ coding is significantly more tolerant with respect to suboptimum receiver bandwidths; using the optimum NRZ receiver bandwidths for RZ reception, we still have an RZ gain of 3.5 dB for $\alpha = 1$, 0.9 dB for $\alpha = 0.4$, and 1.1 dB for the equal rise/fall time signals.

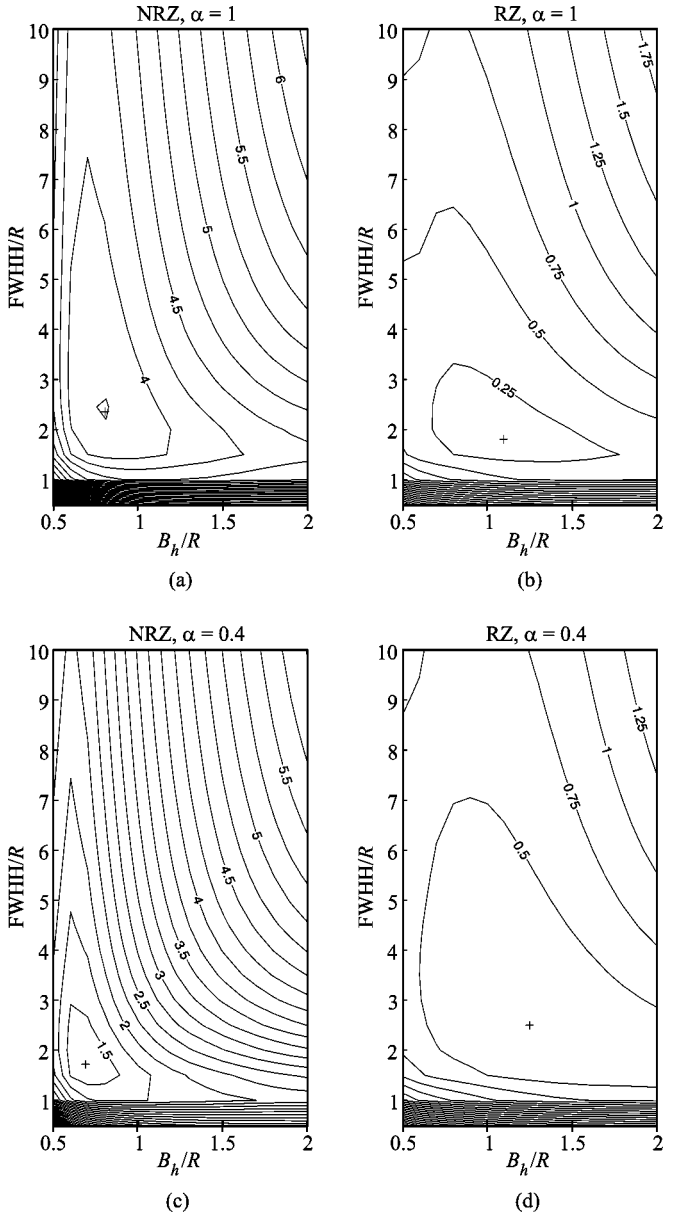


Fig. 3. Sensitivity penalty $\gamma_q$ as a function of normalized FWHH and $B_h$ for optical filtering and BF electrical filtering. (a) and (b) represent NRZ and RZ (33% duty cycle) with $\alpha = 1$, while (c) and (d) were obtained for $\alpha = 0.4$. The contour lines are separated by 0.25 dB, and the crosses indicate the optimum bandwidth constellations.

Comparing the two NRZ input signals, we note that the NRZ signal with steeper edges ($\alpha = 0.4$) yields a significantly higher receiver sensitivity, 2.4 dB above that for NRZ with $\alpha = 1$. The reason for this behavior is twofold. First, the temporally more confined pulses with $\alpha = 0.4$ experience less ISI than those with $\alpha = 1$; for the optimum filter configurations, we find an ISI penalty of 0.5 dB for $\alpha = 0.4$ and of 1.8 dB for $\alpha = 1$. Second, the remaining difference of 1.1 dB reflects the combined effect of smaller receive bandwidths that are made possible by less ISI and considerably cut down detection noise, and of a broader pulse spectrum that better fills the receive characteristics, as detailed in [20].

The surprising, at a first glance, fact that a spectrally three times broader RZ signal may even ask for *narrower* optical fil-

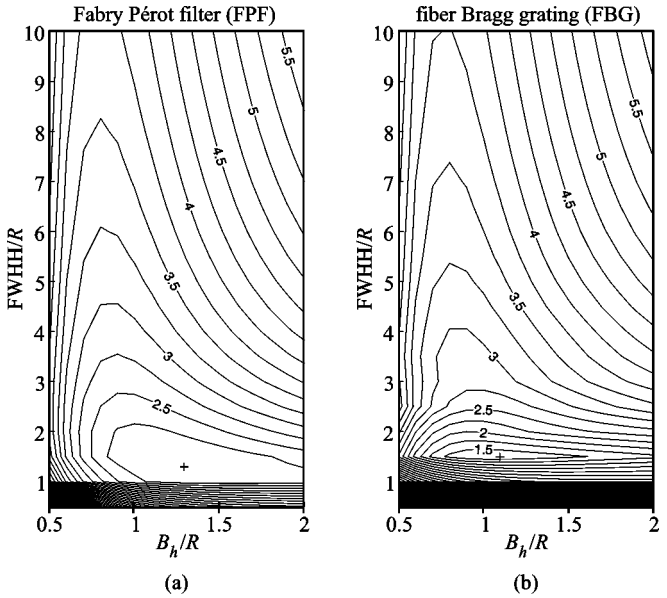


Fig. 4. Sensitivity penalty $\gamma_q$ as a function of normalized FWHH and $B_h$ for NRZ with $\alpha = 0.4$, electrical LF filtering, and (a) optical FPF and (b) an FBG. The contour lines are separated by 0.25 dB, and the crosses indicate the optimum bandwidth constellations.

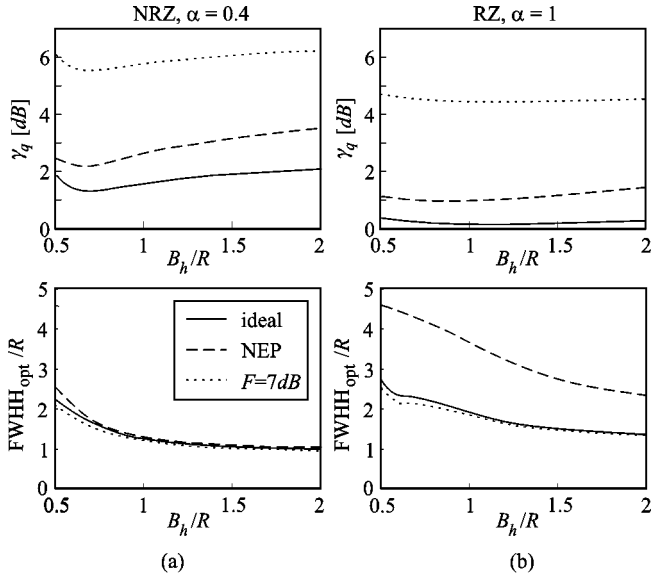


Fig. 5. The upper plots give the sensitivity penalty $\gamma_q$ as a function of the electrical bandwidth $B_h/R$ for optimized optical bandwidths $\text{FWHH}_{\text{opt}}/R$, the latter being shown in the lower plots. Optical FPF filtering and electrical BF filtering is employed, and (a) and (b) apply to NRZ with $\alpha = 0.4$ and 33% duty cycle RZ with $\alpha = 1$, respectively. The solid lines represent an ideal receiver, the dashed lines incorporate the effect of electronic noise ($\text{NEP}/(G\sqrt{R}) = 5 \cdot 10^{-19}$ W/Hz), and the dotted lines illustrate the influence of an enhanced optical amplifier noise figure ($F = 7$ dB).

tering than its NRZ equivalent [cf. Fig. 3(a) and (b)] can also be explained by the different degrading mechanisms. For NRZ, the optimum optical bandwidth is found by trading collected ASE with optical-filter-induced ISI, which sets in noticeably at FWHH $\approx 3.5R$ and FWHH $\approx 2R$ for $\alpha = 1$ and $\alpha = 0.4$, respectively. For RZ, on the other hand, there is no optically induced ISI, and the required balance between signal energy rejection and collected ASE is established at FWHH $\approx 2R$, where almost 30% of the signal energy do not pass the optical filter. The same argumentation holds, both for NRZ and RZ, when interpreting the change in optimum bandwidths going from $\alpha = 1$ to $\alpha = 0.4$. Whereas the accompanying slight spectral broadening causes the optimum bandwidths to *shrink* in the NRZ case due to less ISI, it leads to *broader* optimum bandwidths for RZ in order not to reject too much signal energy.

### C. FPF Versus FBG

When comparing FPF and FBG, the FBG proves to be more sensible to suboptimum bandwidth choices, especially for NRZ. This behavior is visualized by the contour line densities in Fig. 4, where the sensitivity penalty $\gamma_q$ is shown for NRZ with $\alpha = 0.4$, electrical LF filtering, as well as an optical FPF [Fig. 4(a)] and an FBG [Fig. 4(b)]. If the FBG is chosen too narrow, its steep filter edges lead to much higher signal distortions than would be encountered for too narrow an FPF. On the other hand, if chosen slightly too broadband, the FBG collects more ASE while leaving the signal unaffected, whereas increasing the bandwidth of the FPF beyond its optimum value additionally reduces ISI, thus, mitigating the effect of increased ASE. Only for optical bandwidths exceeding $3R$, where the FPF bandwidth has no influence on the signal any longer, the sensitivity decreases by the same amount for the two filters. Due to the better ASE filtering properties, the FBG option shows a sensitivity improvement of 0.7 dB compared to the FPF realization. Since signal distortion is typically not the limiting effect for RZ reception, the two filters behave almost identically for RZ.

## VI. Degrading Effects

We now proceed to study the influence of some important nonideal effects, starting with the incorporation of more realistic receiver noise parameters, i.e., of a limited optical amplifier gain in combination with electronic noise, and of an optical amplifier noise figure exceeding the theoretical limit of 3 dB.

### A. Receiver Noise

Since electronic noise and optical amplifier noise *differently* influence the optimum receiver bandwidths, we first analyze the impact of noisy receive electronics, still assuming an ideal optical amplifier ($F = 3$ dB) with polarization filtering ($M = 1$), an FPF, and a BF. We assume the electronic noise to be specified by the parameter $\text{NEP}/(G\sqrt{R}) = 5 \cdot 10^{-19}$ W/Hz, which corresponds, e.g., to a 10-Gb/s receiver with an equivalent noise current density of 25 pA/$\sqrt{\text{Hz}}$ at the photodiode output, a photodiode sensitivity of 0.8 A/W, and an optical amplifier gain of 28 dB. The results for this scenario are shown in Fig. 5, where Fig. 5 (a) and (b) represent NRZ with $\alpha = 0.4$ and RZ with $\alpha = 1$, respectively. The upper diagrams give the sensitivity penalty $\gamma_q$ with respect to the quantum limit as a function of the electrical bandwidth $B_h/R$ for optimized optical bandwidths $\text{FWHH}_{\text{opt}}/R$, the latter being shown in the lower diagrams. The ideal receiver of Section V is represented by the solid curves, while the dashed lines apply to a receiver degraded by the above specified electronic noise. Noisy electronics lead to a sensitivity degradation of around 1 dB, both for NRZ and RZ reception. A

marked difference between NRZ and RZ is experienced with respect to the optimum *optical* bandwidths, reflecting the two modulation formats' different degrading mechanisms. As evident from the lower plot of Fig. 5(a), in the NRZ case, the optimum optical bandwidths are basically the same as those found for the ideal receiver; the minute tendency toward larger values is due to the fact that (optical-filter-induced) ISI can slightly be reduced by broadening the optical bandpass, while the total detection noise increases only a little due to the presence of a significant electronic noise floor. For RZ, on the other hand, the optimum optical bandwidth nearly doubles compared to the ideal receiver [cf. lower plot of Fig. 5(b)]. The reason is that the presence of electronic noise in addition to the (lower) ASE-ASE beat noise level can be compensated for by letting more signal energy pass the optical filter, until a new balance between signal power and overall detection noise is found.

Let us next assume an optical gain high enough to let electronic noise be no issue, but an equivalent optical amplifier noise figure of $F_{\text{equiv}} = 7$ dB [cf. (5)] and *no* polarization filtering ($M = 2$). The results for this scenario are given by the dotted lines in Fig. 5. The observed sensitivity penalty splits into a 4-dB penalty due to the increased noise figure, and a 0.2- to 0.3-dB penalty due to the higher ASE-ASE beat noise variance. The optimum optical bandwidths are somewhat smaller than for the ideal receiver, *both* for NRZ and for RZ, since the higher (two-polarization) ASE-ASE beat noise asks for compensation by reducing the optical bandwidth.

### *B. Finite Extinction Ratio*

An important reason for suboptimum receiver performance in practical systems is a finite extinction ratio $\zeta$. For NRZ signaling, we define this parameter as the ratio of the maximum optical power for a "1"-bit to the minimum optical power for a "0"-bit. For RZ, we define the extinction ratio as the ratio of the peak optical power for a "1"-bit to the peak optical power for a "0"-bit, since RZ signals are most conveniently generated by passing a primary optical pulse train through a secondary (NRZ) intensity modulator fed by the data signal; the RZ extinction ratio is then determined by the secondary modulator, which will not completely suppress the pulses of the primary pulse train at logical zeros.

Fig. 6(a) shows the influence of the extinction ratio on system performance, expressed in terms of $\gamma_q$, the sensitivity penalty relative to the quantum limit, for an otherwise ideal receiver (cf., Section V). The solid and dashed curves correspond to NRZ with $\alpha = 1$ and $\alpha = 0.4$, respectively, while the dotted curve represents RZ with $\alpha = 1$. Optical and electrical filtering, with bandwidths optimized for perfect extinction, is done by an FPF and a BF. (Optimizing optical and electrical bandwidths for each value of $\zeta$ leads to sensitivity improvements of less than 0.25 dB for the depicted range of $\zeta$.) The horizontal lines give the asymptotic limits for $\zeta \to \infty$. The figure shows that an extinction ratio of $\zeta = 20$ dB causes less than 0.5-dB sensitivity reduction compared to perfect extinction, while the received power nearly has to be *doubled* for $\zeta = 10$ dB, a typical value for today's high-speed intensity modulators. Note that the sensitivity gain of RZ over NRZ only slightly drops with decreasing $\zeta$, which is due to the dominance of signal-dependent noise, as outlined in [20].

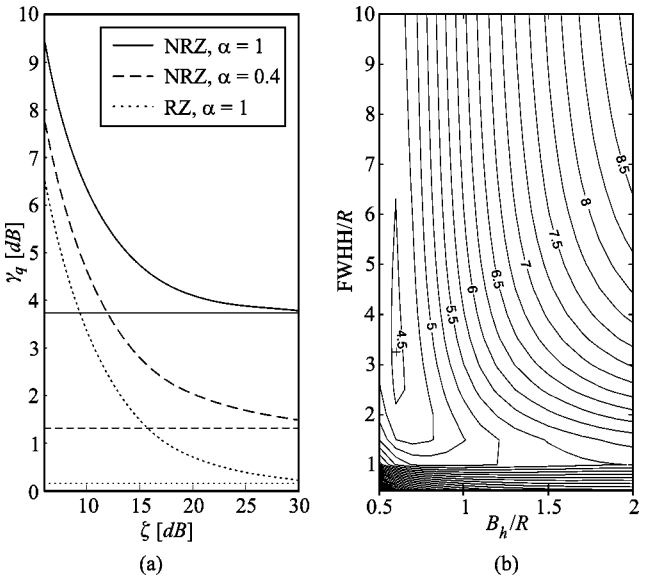


Fig. 6. In (a), the sensitivity penalty $\gamma_q$ as a function of the extinction ratio $\zeta$ is given for optical FPF filtering and electrical BF filtering (solid: NRZ with $\alpha = 1$, dashed: NRZ with $\alpha = 0.4$, dotted: 33% duty cycle RZ with $\alpha = 1$). The horizontal lines represent the asymptotes for perfect extinction. In (b), $\gamma_q$ is shown as a function of the optical and electrical filter bandwidths for NRZ with $\alpha = 0.4$ and $\zeta = 10$ dB; comparison should be made with Fig. 3(c) for the same scenario but with perfect extinction.

TABLE I
OPTIMUM BANDWIDTHS FOR A RECEIVER EMPLOYING OPTICAL FPF FILTERING AND ELECTRICAL BF

| | NRZ, $\alpha = 1$ | | NRZ, $\alpha = 0.4$ | | RZ, $d = 33\%$, $\alpha = 1$ | |
|---|---|---|---|---|---|---|
| | FWHH | $B_h$ | FWHH | $B_h$ | FWHH | $B_h$ |
| $\zeta \to \infty$ | $2.5R$ | $0.8R$ | $1.7R$ | $0.7R$ | $1.8R$ | $1.2R$ |
| $\zeta = 10dB$ | $3.5R$ | $0.7R$ | $3.3R$ | $0.6R$ | $3.1R$ | $0.8R$ |

Fig. 6(b) shows $\gamma_q$ as a function of the optical and electrical filter bandwidths for NRZ with $\alpha = 0.4$ and an extinction ratio of $\zeta = 10$ dB; this figure should be compared to Fig. 3(c) for the same scenario but with perfect extinction. Note that the optimum optical bandwidth increases with decreasing $\zeta$, a behavior that can be explained by considering "0"-bit noise. The poorer extinction ratio implies a higher signal level for the "0"-bits, which, in turn, lets the signal-dependent signal-ASE beat noise rise significantly above the ASE-ASE noise floor for "0"-bit detection. As in the case of high electronic noise (cf. Section V-A), the optical filter may then be increased for less signal distortion, until the growing ASE-ASE beat noise term becomes comparable to the "0"-bit signal-ASE beat noise. At $\zeta = 10$ dB we find the optimum optical/electrical bandwidth constellations given in Table I.

Another interesting aspect that becomes evident comparing Figs. 6(b) and 3(c) is the significant change of the contour lines' shapes: for the lower extinction ratio, the sensitivity is more tolerant with respect to optical bandwidth variations. This feature is due to the fact that the (largely bandwidth-independent) noise-floor given by the "0"-bit signal-ASE beat noise reduces the de-

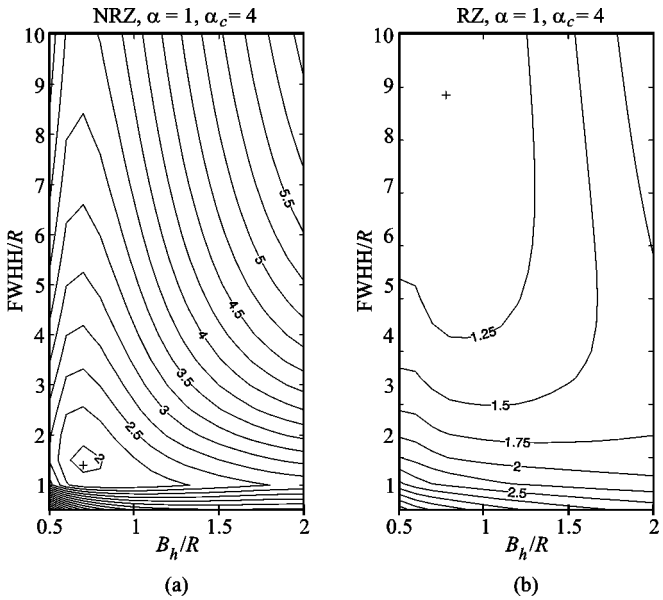


Fig. 7. Sensitivity penalty $\gamma_q$ as a function of normalized FWHH and $B_{li}$ for (a) NRZ and (b) 33% duty cycle RZ with $\alpha = 1$, chirp parameter $\alpha_c = 4$, optical FPF filtering, and electrical BF filtering. The contour lines are separated by 0.25 dB, and the crosses indicate the optimum bandwidth constellations. The figures should be compared to their chirp-free equivalents, Fig. 3(a) and (b).

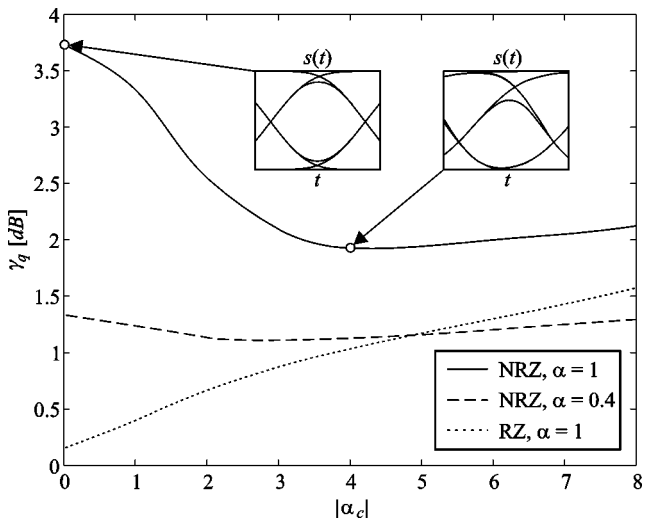


Fig. 8. Sensitivity penalty $\gamma_q$ as a function of the chirp parameter $\alpha_c$ for optimized FPF and BF bandwidths (solid: NRZ with $\alpha = 1$, dashed: NRZ with $\alpha = 0.4$, dotted: 33% duty cycle RZ with $\alpha = 1$). The better performance of chirped NRZ signals is caused by reduced ("0"-bit) ISI, as visualized by the eye diagrams.

teriorating influence of additional ASE-ASE beat noise brought by enlarged optical bandwidths.

### C. Chirp

Most laser intensity modulation techniques employed today introduce a nonlinear phase term (frequency chirp) $\phi(t)$ to the modulated optical field [40]–[43]. Although without direct influence on the optical power waveform at the transmitter, this phase term both broadens the spectrum and leads to signal distortions whenever dispersive elements (such as optical filters!) are involved. In the frame of this work we use the simple chirp model [40]

$$\frac{d\phi(t)}{dt} = \frac{\alpha_c}{2p_{\text{in}}(t)} \cdot \frac{dp_{\text{in}}(t)}{dt} \tag{22}$$

with the chirp parameter $\alpha_c$ being real-valued, constant over time, and typically lying in the range $|\alpha_c| < 5$.

Fig. 7 shows the influence of $\alpha_c$ on the optimum receiver bandwidths for an otherwise ideal receiver using an FPF and a BF; Fig. 7(a) and (b), respectively, apply to NRZ and RZ, both with $\alpha = 1$. This should be compared with Fig. 3(a) and (b), where the corresponding chirp-free curves are shown. It can be seen that for RZ reception, the optical bandwidth must be raised from $1.8R$ to $8.9R$ when going from $\alpha_c = 0$ to $\alpha_c = 4$ for optimum receiver sensitivity. This increase by a factor of nearly 5 owes to the chirp-induced spectral broadening of the input signal,[6] requiring a larger optical filter bandwidth to establish the balance between optical-filter-induced signal energy rejection and detection noise. As the optimum optical bandwidth becomes broader, its (absolute) tolerance to suboptimum values also increases. However, due to the higher ASE-ASE beat noise brought about by the wider optical filter, the performance of RZ coded systems steadily decreases with increasing $\alpha_c$. This behavior is illustrated in Fig. 8, where the dotted line shows the sensitivity penalty $\gamma_q$ relative to the quantum limit as a function of $|\alpha_c|$ for RZ with $\alpha = 1$, for optimized FPF and BF bandwidths.[7]

For NRZ, on the other hand, a chirped signal can even *improve* receiver sensitivity, as indicated by the solid ($\alpha = 1$) and dashed ($\alpha = 0.4$) curves in Fig. 8. For NRZ with $\alpha = 1$, a chirp of $|\alpha_c| = 4$ fully exploits this effect and provides a sensitivity gain of 1.8 dB compared to the corresponding unchirped NRZ signal. This interesting feature owes to the fact that—in contrast to RZ reception—ISI plays a vital role in the case of NRZ [45]. In combination with an optical filter, a chirp can lead to significant NRZ pulse compression, and thus to less ("0"-bit) ISI. This effect is visualized by the eye diagrams in the inserts of Fig. 8; although the eye is slightly more closed for $|\alpha_c = 4|$ than it is for $\alpha_c = 0$, the chirped system performs better, since the compressed NRZ pulses yield significantly less "0"-bit signals and, thus, also less "0"-bit noise. Since NRZ signals with steeper pulse slopes show *a priori* less ISI, this effect is less pronounced for NRZ with $\alpha = 0.4$, as can be seen from the dashed line in Fig. 7. If the chirp is chosen very large, the adverse effect of spectral broadening removes the benefits brought by ISI reduction, and performance deteriorates for the same reasons as in the RZ case. Note from a comparison of Figs. 7(a) and 3(a) that the choice of the optical bandwidth becomes more critical in the chirped case, since filter characteristics and chirp have to be adjusted to each other to provide maximum pulse compression; at optical bandwidths large enough to let the signal field pass undistorted, chirped and unchirped signals yield identical receiver sensitivities, as expected.

### D. Uncompensated Frequency Drifts

Our above analyses show that optical bandwidths of typically twice the data rate lead to optimum receiver performance. However, the choice of such narrow filter bandwidths naturally

[6]Recall that chirped Gaussian pulses show a spectral broadening of $\sqrt{1+\alpha_c^2}$ [3], which, too, applies well to the non-Gaussian RZ pulse shape used here.

[7]Our analyses showed that positive and negative chirp parameters influence $\gamma_q$ alike.

brings up the question of the influence of deviations $\Delta f$ of the transmit laser's frequency relative to the optical filter's center frequency; such deviations can occur in practice due to components' temperature fluctuations or aging, and—in space-borne systems—additionally due to Doppler shifts induced by the satellites' orbital motion. Usually, active frequency-locking circuitry, accompanied by a significant amount of additional system complexity, is employed to partly compensate for such frequency deviations. In this subsection, we answer the question how broad the optical filter should be chosen in the presence of frequency deviations, and what sensitivity penalty has then to be expected.

Frequency fluctuations are slow compared to the data rate. Thus, for a given optical/electrical bandwidth constellation, receiver performance is best characterized by the average number of photons per bit at the receiver input that guarantees BEP $= 10^{-9}$ over the *entire range* of possible frequency deviations $\Delta f \epsilon [-\Delta f_{\max}, \Delta f_{\max}]$, i.e.,

$$n_{s,\,\Delta f_{\max}}(\text{FWHH}, B_h) = \max_{\Delta f} \{n_s(\text{FWHH}, B_h, t_s, s_{\text{th}}, \Delta f)\} \quad (23)$$

where we assume that both sampling instant $t_s$ and decision threshold $s_{\text{th}}$ are kept at their optimum values for $\Delta f = 0$, regardless of the frequency fluctuations. (Our simulations showed that real-time adjustment of $t_s$ and $s_{\text{th}}$, which would require complex electronic circuitry in practice, does not lead to significantly different results.)

Fig. 9(a) shows, for an ideal receiver (cf. Section V), the sensitivity penalty

$$\gamma_0 = n_{s,\,\Delta f_{\max}}/n_{s,\,0} \quad (24)$$

as a function of the maximum frequency deviation $\Delta f_{\max}/R$ if the optical/electrical bandwidth constellation *optimum for zero frequency offset* is employed, irrespective of $\Delta f_{\max}$. The solid and dashed lines apply to NRZ and RZ for FPF optical filtering, whereas the dotted and dashed-dotted lines apply to RZ and NRZ for FBG optical filtering. All examples imply BF electrical filtering and optical signals with $\alpha = 1$. It can be seen that the FPF is more tolerant with respect to frequency fluctuations, a consequence of the fairly moderate dropoff of its transmission characteristics. In contrast, the FBG leads to much higher sensitivity penalties, especially for NRZ, where severe ISI corrupts the optically filtered waveforms in the presence of frequency mismatch. The high sensitivity penalties encountered for optical filtering optimized for zero frequency offset should be compared to Fig. 9(b), where the penalties for the filter constellations yielding optimum performance *over the entire range of frequency shifts* is depicted; note the different scaling of the ordinate axis of Fig. 9(a) and (b). By choosing appropriate optical filter bandwidths, penalties due to frequency drifts can be drastically reduced. The optical bandwidths optimum in the presence of frequency drifts are shown as a function of $\Delta f_{\max}/R$ in Fig. 9(c). It can be seen that enlarging the optical bandwidths from around $2R$ to around $5R$ leads to penalties below 0.6 dB, even for severe frequency offsets on the order of the data rate.[8]

[8]Doppler shifts in typical low-earth orbiting satellite networks may amount so several gigahertz [22].

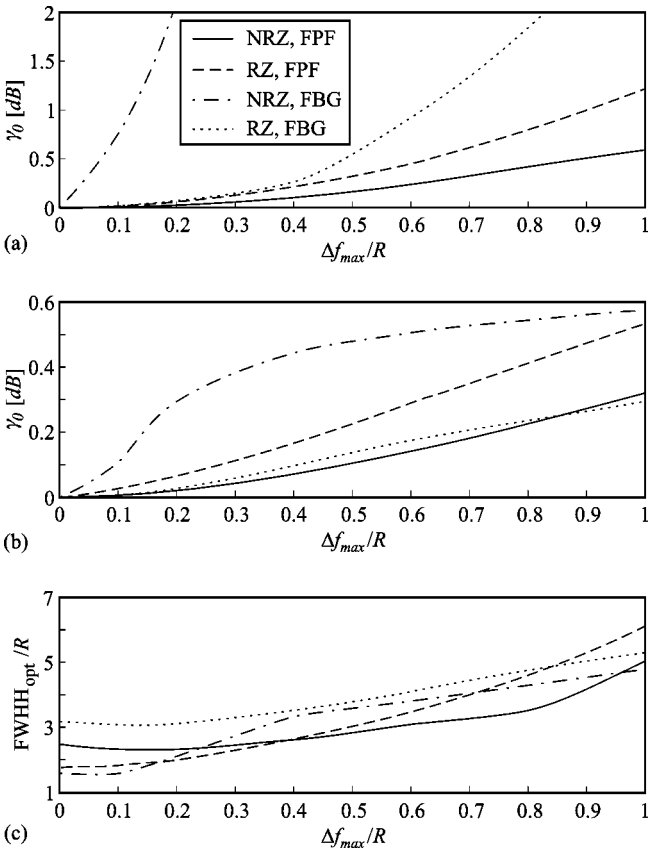


Fig. 9. Sensitivity penalty $\gamma_0$ with respect to each system's ideal performance as a function of the maximum difference $\Delta f_{\max}$ between the optical carrier frequency and the optical filter's center frequency for electrical BF filtering. The solid and dashed curves correspond to NRZ and 33% duty cycle RZ with $\alpha = 1$ and optical FPF filtering, while the dashed-dotted and dotted curves apply to NRZ and 33% duty cycle RZ with $\alpha = 1$ and optical FBG filtering. In (a), the optical/electrical bandwidth constellation *optimum for zero frequency offset* is employed, irrespective of $\Delta f_{\max}$, whereas in (b), the bandwidth constellations are adapted to yield optimum performance *over the entire range of frequency shifts*. The optimum optical bandwidth for each $\Delta f_{\max}$ is given in (c).

This behavior is due to the fact that receiver sensitivity degrades only slightly due to enhanced ASE–ASE beat noise when too large optical filtering is employed, as can be seen in the contour plots of Figs. 2–7.

## VII. Conclusion

We comprehensively analyze the performance of optically preamplified direct detection receivers, both for NRZ and RZ signaling, including realistic optical pulse shapes as well as typical filter transfer functions. Optical FPFs and FBGs, electrical fifth-order BFs, and first-order $RC$ LFs.

We show that for optimum receiver performance, the receiver bandwidths have to be chosen to establish a balance between detection noise and ("0"-bit) *intersymbol interference* (ISI) for NRZ signaling, whereas noise and *filter-induced signal energy rejection* have to be traded for optimum RZ reception. Generally, broader than optimum filtering is to be preferred to too narrow filtering.

Our analyses for *ideal* receivers (characterized by the presence of a single spatial and polarization mode, a 3-dB optical amplifier noise figure, and an optical gain sufficiently large to

let the unavoidable beat noise terms dominate electronic circuit noise) show that—as a consequence of the different trade-offs—the optimum optical bandwidth has to be sought around twice the data rate, *both* for NRZ and the spectrally three times broader RZ signal with 33% duty cycle. This situation changes considerably when *nonideal* effects are included: Electronic noise as well as signal chirp may significantly increase the optimum optical bandwidth in the RZ case, whereas for NRZ the optimum bandwidth is basically left unchanged. Finite extinction ratios, on the other hand, ask for larger optical filter bandwidths for RZ and NRZ alike.

Comparing different optical pulse shapes, our results show that receivers using RZ coding are capable of closely approaching the quantum limit, outperforming NRZ-based systems by several decibels, even if the same optical/electrical bandwidth constellations are used. This RZ gain is largely independent of receiver noise and extinction ratio. (Extinction ratios of around 10 dB reduce receiver sensitivity by typically 3 dB, both for RZ and NRZ.) A comparison of different filter characteristics reveals that using more sophisticated BF electrical filtering instead of LF filtering yields a sensitivity improvement of typically 0.8 dB for NRZ and 0.2 dB for RZ. Optimum electrical bandwidths may differ substanially, especially for NRZ, where the filters' different influence on ISI has to be considered. Employing an FBG instead of an FPF as an optical filter can improve receiver sensitivity by some 0.7 dB for NRZ reception, whereas no improvement is found for RZ.

Pulse chirp always degrades RZ receiver performance, since the chirped pulses' broader spectra require broader optical filtering, which also introduces more detection noise. The performance of NRZ systems, on the other hand, can even be *improved* using chirped pulses, as the interaction of the pulse chirp with the optical filter's phase response can considerably reduce ISI.

If frequency fluctuations between the optical carrier and the optical filter's center frequency are present, the optical bandwidth must be increased; the penalty caused by optical frequency fluctuations on the order of the data rate can be kept below 0.6 dB, if the optical filter bandwidth is chosen about five times the data rate.

## ACKNOWLEDGMENT

The authors wish to acknowledge valuable discussions with K. H. Kudielka.

## REFERENCES

[1] J. C. Livas, "High sensitivity optically preamplified 10Gb/s receivers," in *Proc. OFC'96*, 1996, paper PD4.

[2] P. S. Henry, "Error-rate performance of optical amplifiers," in *Proc. OFC'89*, 1989, paper THK3.

[3] L. Kazovsky, S. Benedetto, and A. Willner, *Optical Fiber Communication Systems*. Norwood, MA: Artech House, 1996.

[4] I. Jacobs, "Effect of optical amplifier bandwidth on receiver sensitivity," *IEEE Trans. Commun.*, vol. 38, pp. 1863–1864, 1990.

[5] N. A. Olsson, "Lightwave systems with optical amplifiers," *J. Lightwave Technol.*, vol. 7, pp. 1071–1082, 1989.

[6] D. Marcuse, "Derivation of analytical expressions for the bit-error probability in lightwave systems with optical amplifiers," *J. Lightwave Technol.*, vol. 8, pp. 1816–1823, 1990.

[7] Y. K. Park and S. W. Granlund, "Optical preamplifier receivers: Application to long-haul digital transmission," *Opt. Fiber Technol.*, vol. 1, pp. 59–71, 1994.

[8] L. F. B. Ribeiro, J. R. F. Da Rocha, and J. L. Pinto, "Performance evaluation of EDFA preamplified receivers taking into account intersymbol interference," *J. Lightwave Technol.*, vol. 13, pp. 225–231, 1995.

[9] S. L. Danielsen, B. Mikkelsen, T. Durhuus, C. Joergensen, and K. E. Stubkjaer, "Detailed noise statistics for an optically preamplified direct detection receiver," *J. Lightwave Technol.*, vol. 13, pp. 977–981, 1995.

[10] M. R. N. Ribeiro, H. Waldman, J. Klein, and L. de Souza Mendes, "Error-rate patterns for the modeling of optically amplified transmission systems," *IEEE J. Select. Areas Commun.*, vol. 15, pp. 707–715, 1997.

[11] D. Ben-Eli, Y. E. Dallal, and S. Shamai (Shitz), "Performance bounds and cutoff rates of quantum limited OOK with optical amplification," *IEEE J. Select. Areas Commun.*, vol. 13, pp. 510–530, 1995.

[12] S. R. Chinn, "Error-rate performance of optical amplifiers with Fabry–Perot filters," *Electron. Lett.*, vol. 31, pp. 756–757, 1995.

[13] I. Tafur Monroy and G. Einarsson, "Bit error evaluation of optically preamplified direct detection receivers with Fabry–Perot optical filters," *J. Lightwave Technol.*, vol. 15, pp. 1546–1553, 1997.

[14] C. Lawetz and J. C. Cartledge, "Performance of optically preamplified receivers with Fabry–Perot optical filters," *J. Lightwave Technol.*, vol. 14, pp. 2467–2474, 1996.

[15] L. Boivin and G. J. Pendock, "Receiver sensitivity for optically amplified RZ signals with arbitrary duty cycle," in *Proc. Optical Amplifiers and Their Applications (OAA'99)*, 1999, paper ThB4, pp. 106–109.

[16] L. Boivin, M. C. Nuss, J. Shah, D. A. B. Miller, and H. A. Haus, "Receiver sensitivity improvement by impulsive coding," *IEEE Photon. Technol. Lett.*, vol. 9, pp. 684–686, 1997.

[17] S. Tanikoshi, K. Ide, T. Onodera, Y. Arimoto, and K. Araki, "High sensitivity 10Gbit/s optical receiver for space communications," in *Proc. 17th AIAA Int. Communications Satellite Systems Conf.*, 1998, pp. 178–183.

[18] W. Atia and R. S. Bondurant, "Demonstration of return-to-zero signaling in both OOK and DPSK formats to improve receiver sensitivity in an optically preamplified receiver," in *Proc. 12th Annu. Meet. LEOS*, 1999, pp. 2244–225.

[19] P. J. Winzer and A. Kalmar, "Sensitivity enhancement of optical receivers by impulsive coding," *J. Lightwave Technol.*, vol. 8, pp. 171–177, 1999.

[20] M. Pauer, P. J. Winzer, and W. R. Leeb, "Bit error probability reduction in direct detection optical receivers using RZ coding," *J. Lightwave Technol.*, vol. 19, pp. 1255–1262, Sept. 2001.

[21] W. R. Leeb, P. J. Winzer, and M. Pauer, "The potential of return-to-zero coding in optically amplified lasercom systems," in *Proc. IEEE Lasers and Electro-Optics Society (LEOS) 1999 Annu. Meet.*, vol. 1, 1999, pp. 224–225.

[22] P. J. Winzer, A. Kalmar, and W. R. Leeb, "Intersatellite laser communication at 1.5$\mu$m: Chances and problems," European Space Agency Contract, Rep. 11 846/96/NL/SB(SC), 1998.

[23] J. C. Livas, E. A. Swanson, S. R. Chinn, and E. S. Kintzer, "High data rate systems for space applications," *Proc. SPIE*, vol. 2381, pp. 38–48, 1995.

[24] S. Yamakawa, T. Araki, and H. Morikawa, "High sensitivity modulation/demodulation scheme for inter-orbit optical communication system with an optical amplifier," in *Proc. IEEE Lasers and Electro-Optics Society (LEOS) 1999 Annu. Meet.*, 1999, paper TuE2, pp. 165–166.

[25] T. Wiesmann and H. Zech, "Optical space communications systems," in *Proc. European Conf. Optical Communications (ECOC)*, 2000, pp. 25–28.

[26] E. Desurvire, *Erbium-Doped Fiber Amplifiers*. New York: Wiley, 1994.

[27] D. E. Johnson, J. R. Johnson, and H. P. Moore, *A Handbook of Active Filters*. Englewood Cliffs, NJ: Prentice-Hall, 1980.

[28] M. Ross, *Laser Receivers*. New York: Wiley, 1966.

[29] B. E. A. Saleh and M. C. Teich, *Fundamentals of Photonics*. New York: Wiley, 1991.

[30] A. Ohtonos and K. Kalli, *Fiber Bragg Gratings*. Norwood, MA: Artech House, 1999.

[31] T. Erdogan, "Fiber grating spectra," *J. Lightwave Technol.*, vol. 15, pp. 1277–1294, 1997.

[32] A. Carbalar and M. A. Muriel, "Phase reconstruction from reflectivity in fiber Bragg gratings," *J. Lightwave Technol.*, vol. 15, pp. 1314–1322, 1997.

[33] G. A. Reider, *Photonik*. Wien/New York: Springer, 1997.

[34] G. Einarsson, *Principles of Lightwave Communications*. New York: Wiley, 1996.

[35] J. Lee and C. Shim, "Bit-error-rate analysis of optically preamplified receivers using an eigenfunction expansion method in optical frequency domain," *J. Lightwave Technol.*, vol. 12, pp. 1224–1229, 1994.

[36] I. Tafur Monroy, "Optically preamplified receiver with low quantum limit," *Electron. Lett.*, vol. 35, pp. 1182–1183, 1999.
[37] P. J. Winzer, A. Kalmar, and W. R. Leeb, "Role of amplified spontaneous emission in optical free-space communication links with optical amplification—Impact on isolation and data transmission; utilization for pointing, acquisition, and tracking," in *Proc. SPIE, Free-Space Laser Communication Technologies XI*, vol. 3615, San Jose, CA, January 23–29, 1999, pp. 134–141.
[38] R. T. Swartz, "High performance integrated circuits for lightwave systems," in *Optical Fiber Telecommunications II*, S. E. Miller and I. P. Kaminov, Eds. San Diego, CA: Academic, 1988.
[39] K. Ogawa, L. D. Tzeng, and Y. K. Park, "Advances in high bit-rate transmission systems," in *Optical Fiber Telecommunications IIIA*, I. P. Kaminov and T. L. Koch, Eds. San Diego, CA: Academic, 1997.
[40] F. Koyama and K. Iga, "Frequency chirping in external modulators," *J. Lightwave Technol.*, vol. 6, pp. 87–92, 1988.
[41] O. Mitomi, S. Nojima, I. Kotaka, K. Wakita, K. Kawano, and M. Naganuma, "Chirping characteristics and frequency response of MQW optical intensity modulator," *J. Lightwave Technol.*, vol. 10, pp. 71–76, 1992.
[42] J. C. Cartledge, "Comparison of effective $\alpha$-parameters for semiconductor Mach–Zehnder optical modulators," *J. Lightwave Technol.*, vol. 16, pp. 372–379, 1998.
[43] P. I. Kuindersma, M. W. Snikkers, G. P. J. M. Cuypers, and J. J. M. Binsma, *et al.*, "Universality of the chirp-parameter of bulk active electro absorption modulators," in *Proc. ECOC'98*, Madrid, Spain, Sept. 1998, pp. 473–474.
[44] P. J. Winzer, "Receiver noise modeling in presence of optical amplification," in *Proc. OAA '01*, 2001, paper OTuE16.
[45] M. M. Strasser, P. J. Winzer, M. Pfennigbauer, and W. R. Leeb, "Significance of chirp for direct-detection free-space laser communications," in *Proc. SPIE*, vol. 4272, 2001.

**Peter J. Winzer** (S'93–A'98) was born in Vienna, Austria, on January 15, 1973. He received the diploma in electrical engineering and the doctorate in technical sciences from the Vienna University of Technology, Vienna, in 1996 and 1998, respectively.

From 1996 to 2000, he was a Research Assistant and Assistant Professor at the Institute of Communications and Radio-Frequency Engineering at the Vienna University of Technology. There, he worked on projects for the European Space Agency on the analysis and modeling of noise in Doppler wind lidar systems, on free-space optical communications, and on optical receivers. Since November 2000, he has been a Member of Technical Staff at Bell Laboratories, Holmdel, NJ.

Dr. Winzer is a member of the Optical Society of America (OSA).

**Martin Pfennigbauer** (S'00) was born in Tulln, Austria, in November 1973. He received the Dipl.Ing. degree in electrical engineering from the Vienna University of Technology, Vienna, Austria, in 2000. He is currently pursuing the Ph.D. degree on laser communication systems.

His research interests include direct detection receivers for NRZ and RZ coding. He is currently involved in a project on optical intersatellite communications.

**Martin M. Strasser** (S'97) was born in Krems, Austria, in June 1974. He received the M.S. degree in electrical engineering from the Vienna University of Technology, Vienna, Austria, in 1998. He is currently pursuing the Ph.D. degree in optical communication systems there.

His research interests include optimum transmitter and receiver designs.

**Walter R. Leeb** received the M.Sc. and Dr.Sc.Techn. degrees in electrical engineering from the Vienna University of Technology, Vienna, Austria.

In the 1970s, he spent two years doing Postdoctoral work for National Aeronautics and Space Administration at Goddard Space Flight Center, Greenbelt, MD. Later, he obtained the Habilitation for Optical Communications and Laser Techniques. He began working at the Institute of Communications and Radio-Frequency Engineering, Vienna University of Technology, as a Lecturer and and has been a Professor there since 1982. Currently, he is head of the institute. His research has included work in the area of optoelectronic devices (laser modulation and laser frequency control) and laser communication system aspects (homodyne and heterodyne receiption, laser synchronization, optical phase-locked loops, intersatellite laser links, space-borne lidar, optical phased array antennas, fiber-optic devices, and high-data rate photonic wavelength multiplexed fiber systems). Most of his space-related work was done for the European Space Agency

Dr. Leeb is a member of the Optical Society of America (OSA).